# Non-fluorinated superamphiphobic surfaces through sol–gel processing of methyltriethoxysilane and tetraethoxysilane

Yuung-Ching Sheen[a], Wei-Hsuan Chang[b], Wen-Chang Chen[b], Yih-Her Chang[c], Yuan-Chang Huang[c], Feng-Chih Chang[a],*

[a] Department of Applied Chemistry, National Chiao Tung University, Hsin Chu 30010, Taiwan
[b] Institute of Polymer Science and Engineering, National Taiwan University, Taipei, Taiwan
[c] Material and Chemical Research Laboratories, Industrial Technology Research Institute, 30050 Hsin Chu, Taiwan

## ARTICLE INFO

## ABSTRACT

In this study, a simple approach was developed to fabricate an extremely superamphiphobic coating material by the tetraethoxysilane (TEOS) and methyltriethoxysilane (MTES) sol–gel derived materials. TEOS and MTES derived moieties were designed for a physical roughness and hydrophobic surface characteristic, respectively. The $^{29}$Si solid-state NMR and ESCA analysis showed the coated silica composition was similar to the feeding ratios of TEOS/MTES. The surface structure characterized from SEM and TEM suggested the nanoparticle-based silica surface was observed at a high TEOS/MTES content but changed to a relatively smooth surface at a low TEOS content. The contact angles of water and $CH_2I_2$ on the pure TEOS derived coated surface were both 0° due to the hydrophilic Si–OH group. As the MTES composition increased to 25 mol% (T5M3), the coated surface had the contact angles of 149.8° and 133.1° for water and $CH_2I_2$, respectively. It revealed that the T5M3-coated surface exhibited both super-hydrophobicity and super-oleophobicity, i.e., superamphiphobicity. Also, it had a relatively low-surface energy (1.38 mJ m$^{-2}$) considerably lower than that of the F-silane-coated surface with 39.3 mJ m$^{-2}$. As the MTES composition increased further, both contact angles of water and $CH_2I_2$ decreased. Especially, they decreased dramatically at the MTES feeding composition higher than 75 mol%, due to the much less rough surface at a higher MTES composition. The present study suggests that superamphiphobic surface could be achieved by non-fluorinated sol–gel derived silica materials.

© 2008 Published by Elsevier B.V.

## 1. Introduction

Lotus effect is a well-known super-hydrophobic phenomenon observed in nature [1,2]. Combination of chemically hydrophobic waxy surface and physically rough micro- and nanoscale binary structure leads to the self-cleaning properties of the lotus leaf. Such super-hydrophobic phenomena was simulated by various chemical or physical surface treatments [4–17]. For example, flat man-made surfaces modified by fluoropolymers or silanes as low-surface energy modifiers led to water contact angles as high as 120° [3]. Recently, super-hydrophobic surfaces based on organic-modified silica nanoparticle were discovered to have water contact angle larger than 150° [16–20]. They were resulted from roughness based on the nanoparticle size and hydrophobic characteristic of organic moiety. The organic-modified materials included low-surface-free-energy polybenzoxazine [16,20] and fluoroalkylsilane [17–19]. However, the above organic-modified surfaces required extra organic reaction on nanoparticles and could be difficult to control the surface characteristics. Also, fluoro-materials was expensive and thus limited its commercial application. A direct sol–gel reaction to produce organic-modified nanoparticles without fluoroalkylsilane would be a simple process for obtaining superamphiphobic surfaces.

In this study, superamphiphobic surfaces prepared from the tetraethoxysilane (TEOS) and methyltriethoxysilane (MTES) sol–gel derived coating materials were explored, as shown in Scheme 1. First, sol–gel reaction on different compositions of TEOS/MTES was carried out to form the primary particle, then further gelation on

* Corresponding author at: Department of Applied Chemistry, National Chiao Tung University, Science Building 2, Hsin Chu 30010, Taiwan.
Tel.: +886 3 5131512; fax: +886 3 5723764.
E-mail address: changfc@mail.nctu.edu.tw (F.-C. Chang).
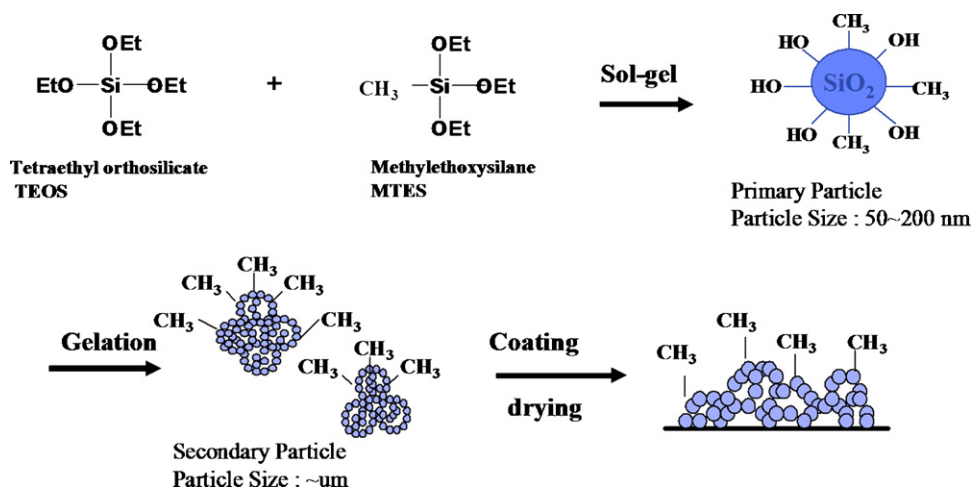
**Scheme 1.** Proposal mechanism of the superamphiphobic surface formed by TEOS/MTES sol–gel derived coating.

**Table 1**
Contact angles and surface energies of photographic paper coated with different TEOS/MTES sol–gel derived silica solution.

| Sample | MTES (mol%) | Carbon[a] content (at.%) | H₂O contact angle (°) | CH₂I₂ contact angle (°) | Surface free energy $\gamma$ (mJ m⁻²) |
|---|---|---|---|---|---|
| Unmodified paper (blank) | 0.0 | – | 36.1 | 0 | 66.9 |
| F-silane-coated paper | 0.0 | – | 107.5 | 48.3 | 39.3 |
| T1M0 | 0.0 | 8.0 | –[b] | –[b] | – |
| T7M1 | 12.5 | 17.9 | 151.9 | –[b] | – |
| T3M1 | 25.0 | 21.0 | 146.2 | 35.6 | 72.42 |
| T5M3 | 37.5 | 23.5 | 149.8 | 133.1 | 1.38 |
| T1M1 | 50.0 | 26.4 | 147.0 | 120.8 | 3.64 |
| T3M5 | 62.5 | 27.6 | 147.0 | 114.9 | 5.50 |
| T1M3 | 75.0 | 32.3 | 95.4 | 68.7 | 23.93 |
| T1M7 | 87.5 | 33.2 | 95.0 | 64.8 | 25.97 |
| T0M1 | 100.0 | 35.5 | 98.3 | 65.3 | 25.54 |

[a] The carbon content (at.%) by the measurement of ESCA.
[b] The liquid drop was immediately absorbed by the rough surface.

the above reaction product by adding ammonium hydroxide led to the secondary particle in solution. Next, the above sol–gel solution was coated onto photographic paper substrate and followed by drying to form the superamphiphobic surfaces. TEOS derived silica was designed for a physical roughness of micro- and nanoscale binary structures and MTES for improving hydrophobic surface characteristic. The chemical compositions of the sol–gel derived materials were analyzed by solid-state NMR and ESCA. Effects of the MTEO/TEOS composition on the morphology and surface characteristic were investigated by SEM, AFM, and contact angle measurements. The experimental results suggested such simple non-fluoroalkyl silica could produce the superamphiphobic surfaces with the contact angle of water or diiodomethane higher than that of fluoropolymer.

## 2. Experimental

### 2.1. Materials

TEOS and MTES were obtained from Acros (New Jersey, USA) and used without further purification. Tridecafluoro-1,1,2,2,-tetrahydrooctyl-1-triethoxysilane(1H,1H,2H,2H-perfluorooctyltriethoxysilane) was supplied by the Seedchem Co. (Melbourne, Australia). 2-Amino-2-methyl-propanol (AMP95) was supplied by Neuto Products Co. (Taipei, Taiwan). Ammonium hydroxide (28 wt%) was gained by Showa (Tokyo, Japan). Diiodomethane was supplied by Lancaster (Lancashire, UK). Isopropyl alcohol (IPA), ethanol and acetic acid were supplied by the Tedia Chemical Co. (Fairfield, USA).

### 2.2. Preparation of TEOS/MTES sol–gel solution

A mixture of different compositions of TEOS and MTES [molar fractions ranging from 1:0 to 0:1 (Table 1); total: 0.0192 mol], AMP95 (2.26 g), ethanol (21 g), and DI water (1.05 g), were added to 50 ml capped glass bottle under vigorous stirring at room temperature for 1 h. Then, another 2.26 g of ammonium hydroxide (28 wt% in water) was added under vigorous stirring at room temperature for 6 h. As examples of the nomenclature used in this study, T1M0 and T7M1 refer to the samples prepared from 1:0 and 7:1 molar ratios of TEOS and MTES for preparing the above precursor solutions, respectively.

### 2.3. Preparation of superamphiphobic surfaces

The above TEOS/MTES sol–gel derived silica solution (in ethanol) were coated onto a photographic paper (purchased from Printer Co., Taiwan) by doctor blade
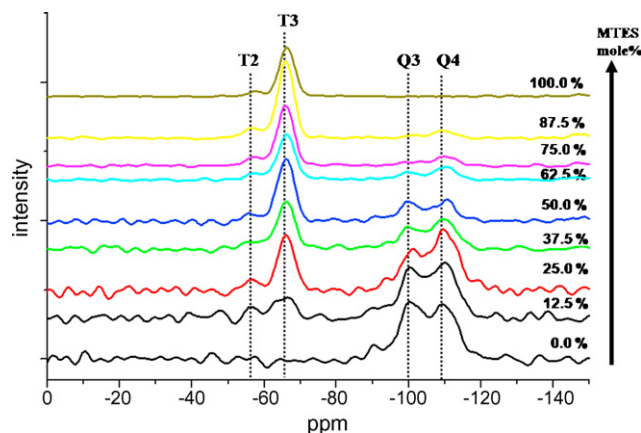


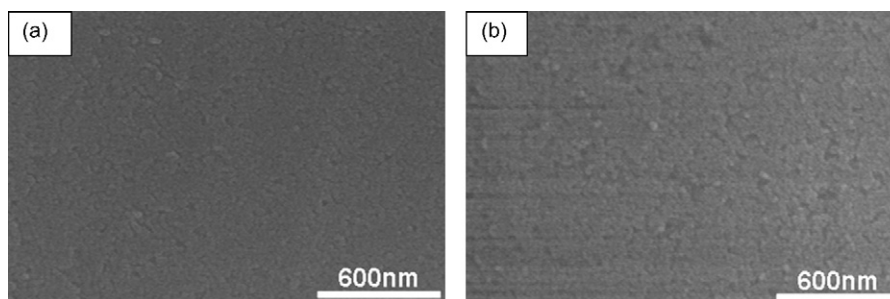**Fig. 1.** Solid-state ²⁹Si NMR spectra of the sol–gel derived silica from different TEOS/MTES compositions.

**Fig. 2.** SEM images of the (a) blank and (b) F-silane-coated photographic paper substrate.
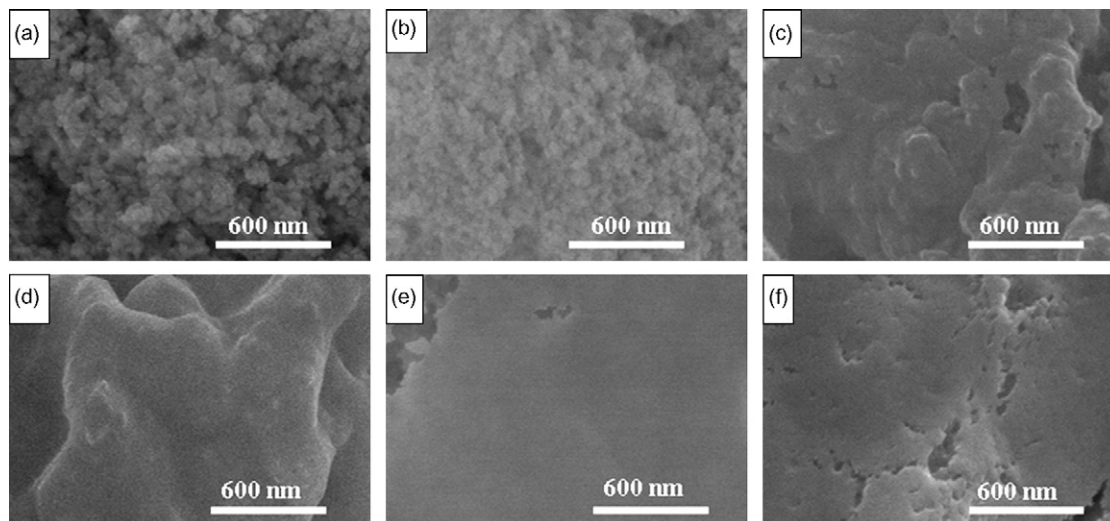


**Fig. 3.** SEM images (50,000×) of the surfaces of the photographic paper substrates coated with the composition and MTES (mol%): (a) T1M0 (0%); (b) T7M1 (12.5%); (c) T3M1 (25%); (d) T1M1 (50%); (e) T1M3 (75%); (f) T1M7 (87.5%) silica.

and put into oven for drying at 120 °C for 1 h to form the super-hydrophobic and superamphiphobic silica surfaces. The coated silica thickness on the surface was around 500 μm.

### 2.4. Preparation of F-silane-coated surface for comparison

A mixture of 1H,1H,2H,2H-perfluorooctyltriethoxysilane (0.95 g (0.00185 mol)), IPA (30 g), DI water (1.58 g), and acetic acid (100 μl, 0.00175 mol) were added to 50 ml of capped glass bottle under vigorous stirring at room temperature for 24 h. The above F-silane (PFS) solution was then coated onto a photographic paper substrates by dipping process and put into oven at 120 °C for 1 h to obtain the PFS coated surface.

### 2.5. Characterization

Solid-state $^{29}$Si NMR spectra were recorded at room temperature using a Bruker AM 500 spectrometer. The sample was ground to a fine powder and then placed into the NMR tube. Chemical compositions of the substrate surface were analyzed using a Thermo VG Scientific ESCALAB 250 spectrometer equipped with a monochromatic Al Kα X-ray source (1486.6 eV photons), the vacuum in the analysis chamber was maintained at ca. 10–8 mbar or lower.

Microstructure of the prepared silica surfaces was characterized using a Hitachi S-4200 scanning electron microscope. Atomic force microscopy (AFM) images were acquired using a Veeco MultiMode scanning probe microscope. Damage to both the tip and the sample surface was minimized by employing the AFM in the tapping mode. The values of root-mean-square (RMS) roughness were calculated over scan area of 10 μm × 10 μm.

The static contact angles of 5-μl liquid drops deposited on the silica surfaces were determined through contact angle goniometry at 25 °C using an AST Products Optima XE goniometer (Billerica, USA) interfaced with image-capture software. To obtain reliable contact data, at least three droplets were placed on different regions of at least two pieces of film. The surface free energy was estimated according to those reports by Owens and Wendt [21] and Kaelble and Uy [22] and given below briefly. The work equation extended from Fowkers' equation to a geometric mean

method is given by

$$\gamma_i(1 + \cos \theta_i) = 2 \left( \sqrt{\gamma_i^d \gamma_s^d} + \sqrt{\gamma_i^p \gamma_s^p} \right), \quad i = 1, 2 \tag{1}$$

$\theta_i$ and $\gamma_i$ refer to contact angle and surface free energy of liquid 1 and liquid 2, respectively. $\gamma_i^d$, $\gamma_i^p$, $\gamma_s^d$ and $\gamma_s^p$ are assumed to refer to dispersion (nonpolar) forces and polar (nondispersion) forces between the liquid and solid phases.

## 3. Results and discussion

Fig. 1 exhibits the solid-state $^{29}$Si NMR spectra of the TEOS/MTES derived materials. The peak positions of Q4, Q3, T3, and T2 of TEOS/MTES derived materials are observed at −109.3, −100.3,
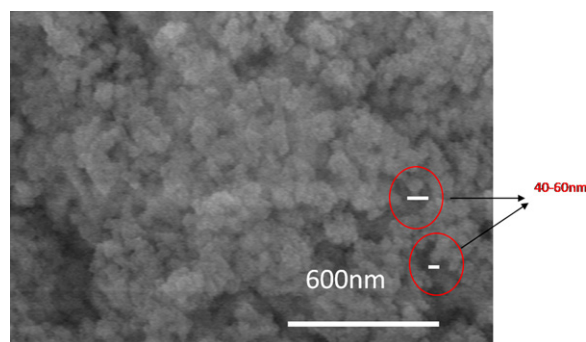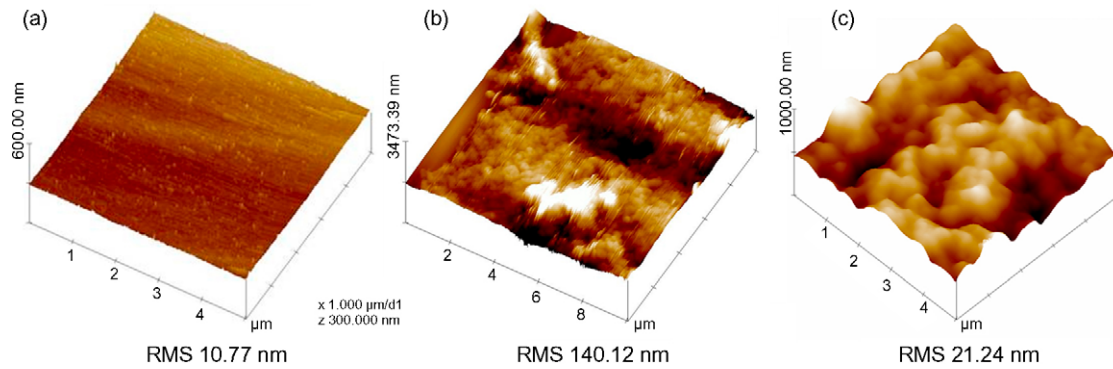


**Fig. 4.** SEM image of the surfaces of the photographic paper substrates coated with the sol–gel derived material, T1M0 (0%).

**Fig. 5.** AFM images of the (a) blank photographic paper and photographic paper coated with the sol–gel derived silica from the composition and MTES (mol%), (b) T3M5 (37.5%), and (c) T1M3 (75%).

−66.2 and −57.0 ppm, respectively, which are similar to those reported in the literature. As shown in Fig. 1, the peak intensities of the Q3 and Q4 decrease with increasing the MTES content while the peak intensities of T2 and T3 show a reverse trend. It suggests that the synthesized material compositions are similar to those of the feeding mole ratios of TEOS/MTES.

The TEOS/MTES silica derived composition on surface was further characterized by ESCA. We observed photoemission peaks from the F 1s, O 1s, C 1s, and Si 2p core levels together with Auger structures related to elemental carbon, oxygen, and fluorine species. In the following, the atomic percentage of carbon (Table 1) was estimated from the elemental concentrations represented by
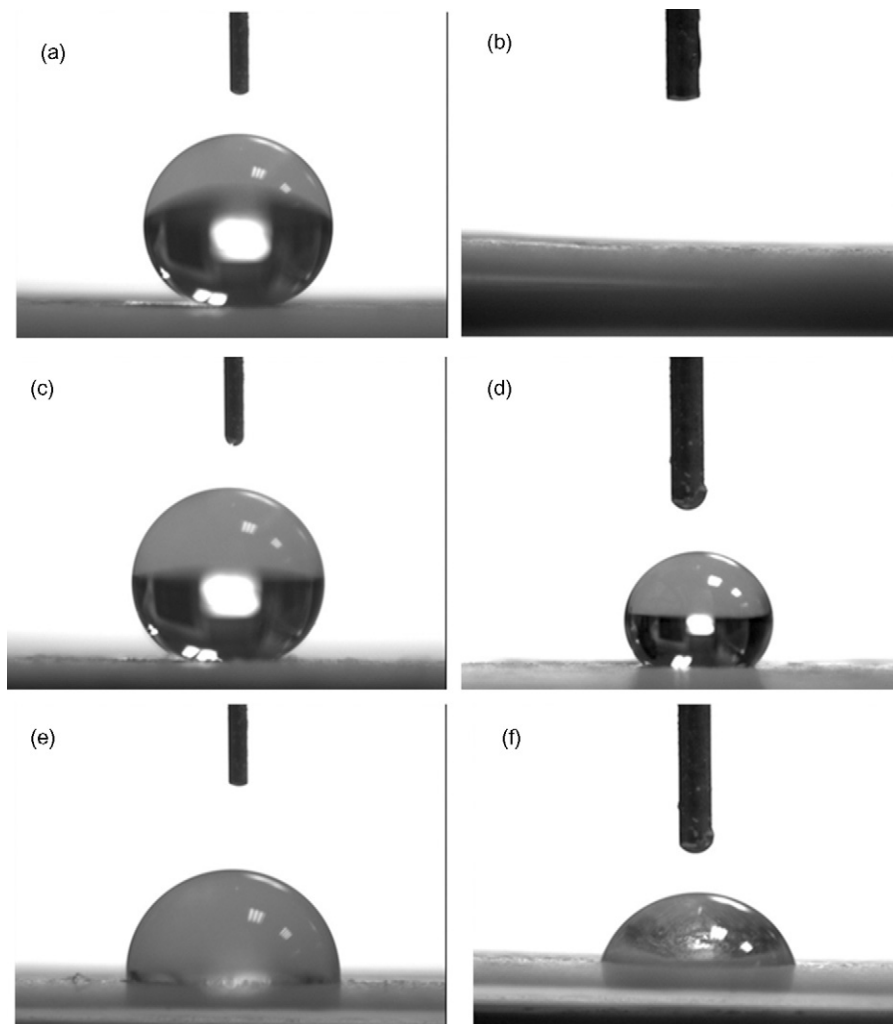


**Fig. 6.** Photographs of liquids water (5 μl) placed on the silica-coated substrate and the composition and MTES (mol%): (a) T7M1 (12.5%), (c) T5M3 (37.5%), and (e) T0M1 (100%); CH$_2$I$_2$ (5 μl) on the silica-coated substrate: (b) T7M1 (12.5%), (d) T5M3 (37.5%), and (f) T0M1 (100%).
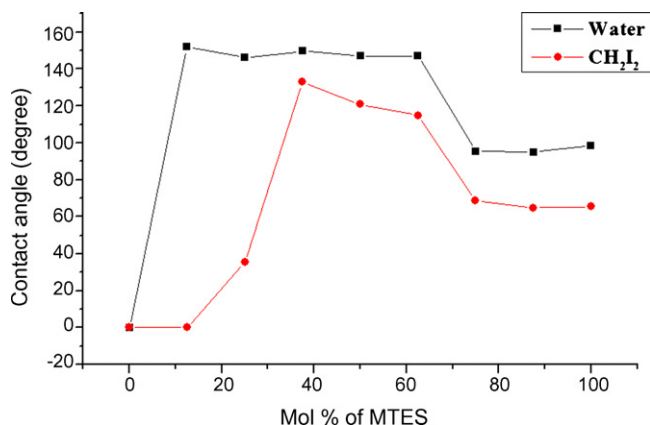
**Fig. 7.** Contact angles of photographic paper substrates coated with sol–gel derived silica from different compositions of TEOS/MTES.

the C 1s, O 1s, F 1s, and Si 2p core energy levels. The obtained carbon content vary from 0 to 35.5 at.% as the MTES feeding composition increases from 0% (T1M0) to 100% (T0M1). It again shows that the coated composition on the surface is on the trend as the original feeding composition.

The surface structures were analyzed by SEM and AFM. As a basis for comparison, the surface characteristics of the blank paper substrate and F-silane-coated surface were studied first. Fig. 2(a) and (b) shows the SEM images of the blank and F-silane-coated photographic papers, respectively. Both images are smooth with contact angles of 36.1° and 107.5° for water, respectively, while the corresponding surface free energies of 66.9 and 39.3 mJ m$^{-2}$. It is as expected that the F-silane-modified surface of the photographic paper had a higher contact angle and a lower surface energy than the blank.

Fig. 3 shows the SEM images (50,000×) of the photographic paper coated with the different compositions of sol–gel derivated silica: (a) T1M0; (b) T7M1; (c)T3M1; (d) T1M1; (e) T1M3; (f) T1M7, respectively. As shown in Fig. 4, silica nanoparticle with the estimated sizes around 40–60 nm is clearly observed. Such nanoparticle-based rough surface gradually becomes smooth as the MTES content increases. Note that the SEM image of the T0M1 coated sample could not be obtained due to the poor film quality. Fig. 5 shows the AFM images of the (a) blank paper substrate, that coated with the (b) T3M5, and (c) T1M3 sol–gel derived silica. The root-mean-square surface roughness estimated from the above AFM images are 10.77, 140.12, and 21.24 nm, respectively. It suggests that a lower TEOS/MTES ratio leads to a less rough surface. The above variation on the SEM and AFM images is explained as below. Silica nanoparticles synthesized from tetra-functional TEOS sol–gel reaction generally exhibits a three-dimension microstructure with hydrophilic OH groups on the surfaces. However, the tri-functional MTES may have a two-dimension planar structure with hydrophobic CH$_3$ groups on the silica surfaces. Such variation on the surface structure would be important for obtaining optimum TEOS/MTES composition to create the superamphiphobic surface.

The static contact angle measurement was used to characterize the hydrophobicity and oleophobicity of the TEOS/MTES derived silica surfaces. Contact angle measurements reflect the characteristics of the interface between the coating film and the probe liquid, including both the thermodynamic parameters and the surface roughness. In this measurement, drops of water and CH$_2$I$_2$ were placed directly upon the rough surfaces, as shown in Fig. 6. The variation of contact angle with different TEOS/MTES coating compositions is shown in Fig. 7 and Table 1. The contact angles of water and CH$_2$I$_2$ on the T1M0-coated film were both 0° (i.e.,

complete wetting of the surface), due to the hydrophilic Si–OH group on the surface. Interestingly, a dramatic increase on the water contact angle of 151.9° is observed for the T7M1-coated surface (note that a value greater than 150° corresponds to super-hydrophobicity). However, the static contact angle for CH$_2$I$_2$ was 0° for the T7M1-coated surface due to the presence of the hydrophobic CH$_3$ groups of the MTES moiety. As the MTES composition increased to 25 mol%, the T5M3-coated surface had the contact angles of 149.8° and 133.1° for water and CH$_2$I$_2$, respectively. It reveals that the T5M3-coated surface exhibits both super-hydrophobicity and super-oleophobicity, i.e., superamphiphobicity, resulted from the rough TEOS-derived surface and hydrophobic MTES-derived surface. Also, it has a relatively low-surface energy (1.38 mJ m$^{-2}$) considerably lower than that of F-silane-coated surface with 39.3 mJ m$^{-2}$. As the MTES composition increases further, both contact angles of water and CH$_2$I$_2$ decrease. Especially, they decrease dramatically at the MTES feeding composition higher than 75 mol%. It can be explained by the much less rough surface at a higher MTES composition, as observed from SEM and TEM images. Nevertheless, the T0M1 (100% MTES feeding composition) possessed a low-surface energy of 25.54 mJ m$^{-2}$, very close to the surface energy of the fluoropolymer poly(tetrafluoroethylene) (ca. 20–21 mJ m$^{-2}$).

## 4. Conclusions

We have successfully developed a simple approach to fabricate an extremely superamphiphobic coating material by the TEOS/MTES sol–gel derived materials. The coated silica composition was similar to the feeding ratios of TEOS/MTES. The surface structure showed the nanoparticle-based silica surface was observed at a high TEOS/MTES content but changed to a relatively smooth surface at a low TEOS content through the optimization of the TEOS/MTES composition, the T5M3-coated surface with 25 mol% of MTES had the contact angles of 149.8° and 133.1° for water and CH$_2$I$_2$, respectively. It exhibited both super-hydrophobicity and super-oleophobicity, i.e., superamphiphobicity, resulted from the rough TEOS-derived surface and hydrophobic MTES-derived surface. Also, it has a relatively low-surface energy (1.38 mJ m$^{-2}$) considerably lower than that of F-silane-coated surface with 39.3 mJ m$^{-2}$. The present study suggests that superamphiphobic surface could be achieved by non-fluorinated sol–gel derived silica materials.

## Appendix A. Supplementary data

Supplementary data associated with this article can be found, in the online version, at doi:10.1016/j.matchemphys.2008.07.132.

## References

[1] C. Neinhuis, W. Barthlott, C. Neinhuis, Ann. Bot. 79 (1997) 667.
[2] W. Barthlott, C. Neinhuis, Planta 202 (1997) 1.
[3] E.G. Shafrin, W.A. Zisman, Contact angle, wettability, and adhesion, in: F.M. Fowkes (Ed.), Advances in Chemistry Series, vol. 43, American Chemical Society, Washington, DC, 1964, p. 145.
[4] X.J. Feng, J. Zhai, L. Jiang, Angew. Chem. Int. Ed. 44 (2005) 5115.
[5] M.H. Jin, X.J. Feng, L. Feng, T.L. Sun, J. Zhai, T.J. Li, L. Jiang, Adv. Mater. 17 (2005) 1977.
[6] M. Morra, E. Occhiello, F. Garbassi, Langmuir 5 (1989) 872.
[7] I. Woodward, W.C.E. Schofield, V. Roucoules, J.P.S. Badyal, Langmuir 19 (2003) 3432.
[8] K. Tsujii, T. Yamamoto, T. Onda, S. Shibuichi, Angew. Chem. Int. Ed. Engl. 9 (1997) 36.
[9] T. Onda, S. Shibuichi, N. Satoh, K. Tsujii, Langmuir 12 (1996) 2125.
[10] L. Gao, T.J. McCarthy, Langmuir 24 (2008) 362.
[11] H. Yan, K. Kurogi, H. Mayama, K. Tsujii, Angew. Chem., Int. Ed. 44 (2005) 3453.
[12] X. Yu, Z. Wang, Y. Jiang, F. Shi, X. Zhang, Adv. Mater. 17 (2005) 1289.
[13] F. Xia, L. Feng, S. Wang, T. Sun, W. Song, W. Jiang, L. Jiang, Adv. Mater. 18 (2006) 432.

[14] F. Shi, Z. Wang, X. Zhang, Adv. Mater. 17 (2005) 1005.
[15] L. Zhai, C. Fevzi, R.E. Cohen, M.F. Rubner, Nano Lett. 7 (2004) 1349.
[16] C.F. Wang, Y.T. Wang, P.H. Tung, S.W. Kuo, C.H. Lin, Y.C. Sheen, F.C. Chang, Langmuir 22 (2006) 8289.
[17] J. Bravo, L. Zhai, Z. Wu, R.E. Cohen, M.F. Rubner, Langmuir 23 (2007) 7293.
[18] M. Hikita, K. Tanaka, T. Nakamura, T. Kajiyama, A. Takahara, Langmuir 21 (2005) 7299.
[19] H.M. Shang, Y. Wang, K. Takahashi, G.Z. Cao, J. Mater. Sci. 40 (2005) 3587.
[20] C.F. Wang, S.F. Chiou, F.H. Ko, C.T. Chou, H.C. Lin, C.F. Huang, F.C. Chang, Macromol. Rapid Commun. 27 (2006) 333.
[21] D.K. Owens, R.C. Wendt, J. Appl. Polym. Sci. 13 (1969) 1741.
[22] D.H. Kaelble, K.C. Uy, J. Adhes. 2 (1970) 50.